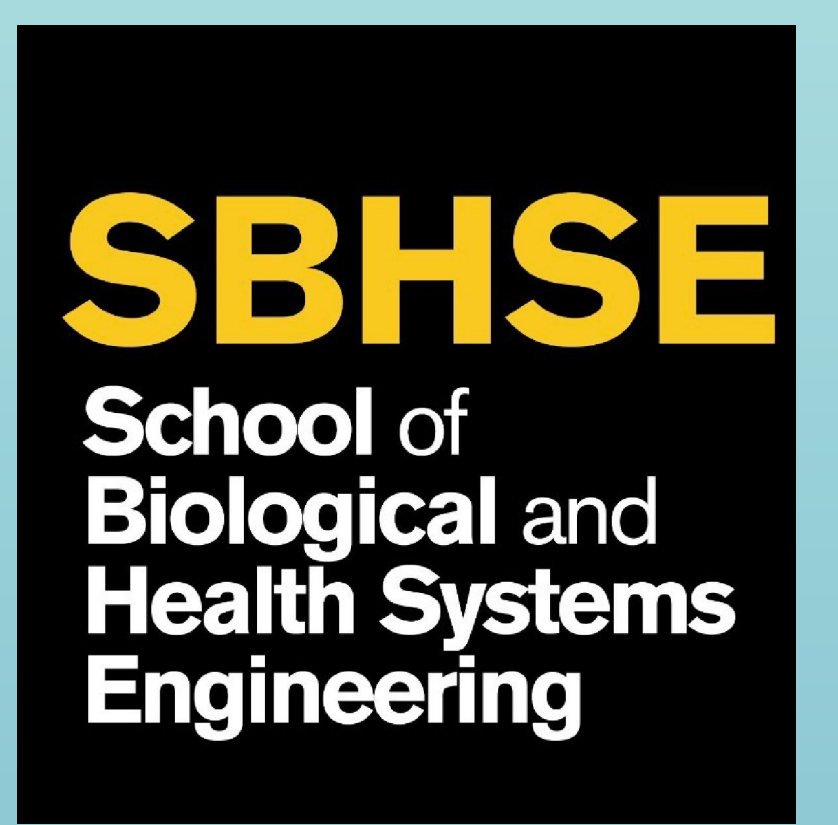




## Technology (SCOUT)

Jenna Materna<sup>1</sup>, Solenne Norvor-Davis<sup>1</sup>, Maya Sampath<sup>1</sup>, Kiernan Sutton<sup>1</sup>  
 Dr. Sung-Min Sohn, PhD<sup>1</sup>, Dr. Michael Pham, MD<sup>2</sup>, Dr. Vivek Najaraja, MBBS, MD<sup>2</sup>  
 School of Biological and Health Systems Engineering, Arizona State University<sup>1</sup>,  
 Division of Rheumatology, Mayo Clinic Arizona<sup>2</sup>



### Clinical Problem



Calcinosis is a common and debilitating condition secondary to systemic sclerosis (SSc), affecting up to one quarter of patients and leading to **pain, ulceration, infection, and functional impairments**[1]-[3]. Current imaging modalities, are limited by operator dependence, lack of three-dimensional quantification, and suboptimal sensitivity for small or deep lesions [4]-[8]. There is a critical need for **noninvasive, point-of-care technologies** that can reliably **detect, quantify, and map calcinosis in SSc**, particularly in the hands and forearms where disease burden is highest [1][2]. Recent advances in **wearable ultrasound technology, including flexible, stretchable, and hydrogel-based transducer arrays**, have enabled continuous, operator-independent imaging with high spatial resolution and tissue conformity, but have not yet been applied to SSc-related calcinosis [9]-[11].

### Mission Statement

We aim to innovate a viable device that will help with the diagnosis and treatment of patients suffering from calcinosis. We, as a group, value **innovation, integrity, and quality**, all of which are critical in our mission to develop our device. Together, alongside our patients and mentors, we are committed to **closing the gaps in healthcare access for underserved communities** and ensuring **medical solutions are equitable and accessible to all**.

### Market Analysis

Currently, calcinosis affects **40% of patients with SSc**, estimating at roughly **2.5 million people worldwide**. The market for SSc is estimated at **USD 2.74 billion in 2025** and has an anticipated compound annual growth rate (CAGR) of **5.07% from 2025 to 2034** [13].

### Product Specifications

Category	Specification	Customer Need
Acoustic Properties	Acoustic impedance: $1.6 \times 10^6 \text{ kg/m}^2 \cdot \text{s}$	Clear, high-quality ultrasound imaging
Electrical Impedance	$50 \Omega \pm 10 \Omega$	Reliable signal performance without artifacts
Phase Requirements	Phase $\approx 0^\circ$ at probe center; $-15^\circ \leq \arg(Z_{\square}) \leq +15^\circ$ across 2–15 MHz	Consistent, accurate imaging across frequency range
Waveform Constraints	Nearly resistive load; minimal waveform distortion	Precise diagnostic imaging with reduced distortion
Hydrogel Operating Conditions	Pressure $\leq 5 \text{ kPa}$ ; Temperature $< 37^\circ\text{C}$	Comfortable, safe use on sensitive scleroderma-affected hands
Safety Features	Heat sensor; auto shut-off to prevent overheating	Prevents burns or discomfort; ensures safe home/clinical use
Probe Ergonomics	Non-slip handle; adjustable wide-grip	Easy handling for patients with limited hand mobility or stiffness
Hydrogel Composition	Primarily <b>Polyurethane (PU) gel</b>	Durable, flexible, and biocompatible contact material
Hydrogel Thickness	10 mm	Adequate coupling for consistent image quality
Sleeve Dimensions	9 in length $\times$ 4 in width	Fits a wide range of hand sizes comfortably

### Product Concept and Design

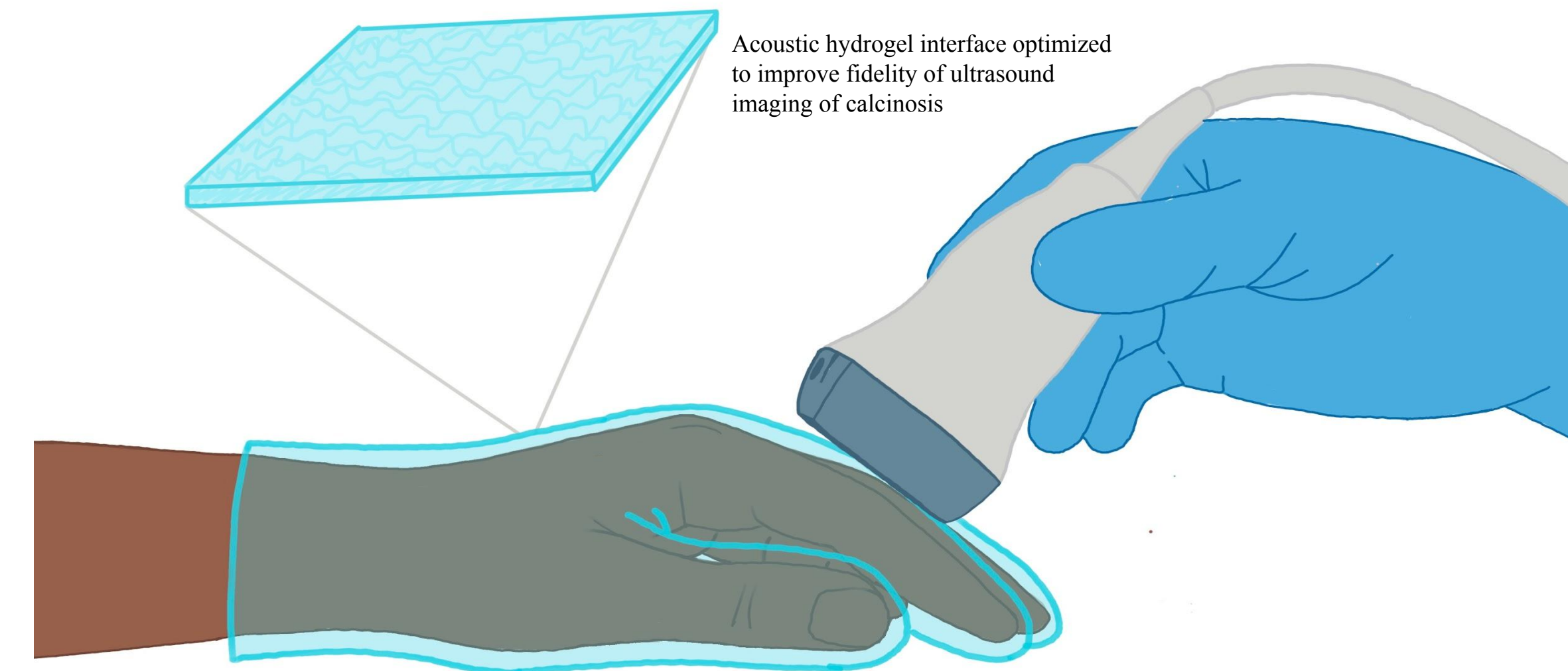


**Figure 1.** The product concept is composed of a hydrogel material chemically modified to improve the fidelity of ultrasound imaging of calcinosis deposits. The hydrogel material will be tuned to match the electric impedance of the skin and soft tissue, minimize reflection or noise caused by the presence of calcium in the skin, and be adaptable to existing ultrasound workflows to minimize burdens to clinical integration.

### Virtual Prototyping

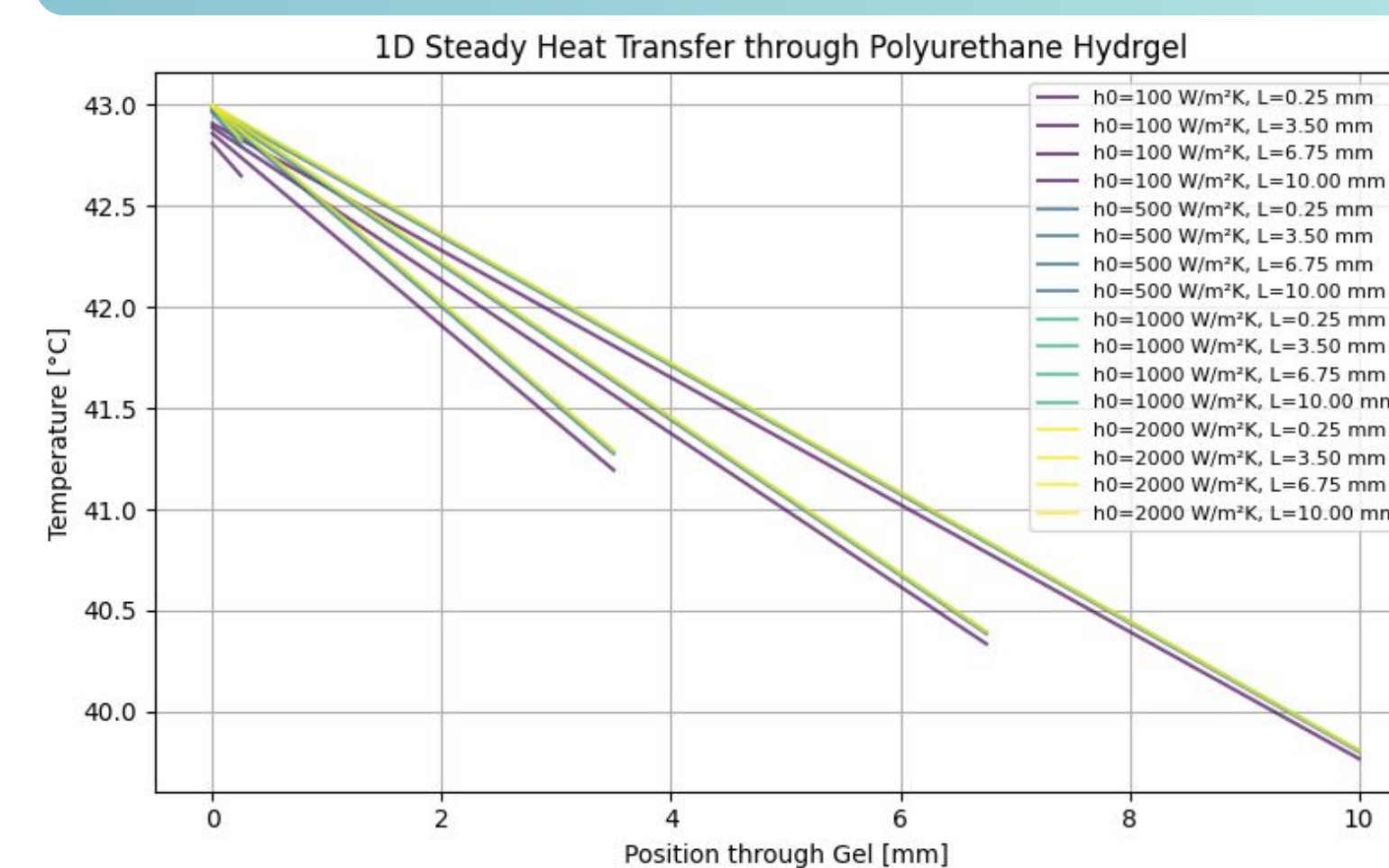


**Figure 2.** Sample graphical representation of the heat transfer through the gel. Multiple iterations with varying thicknesses and convective heat transfer coefficients are shown in this Temperature vs Position plot.

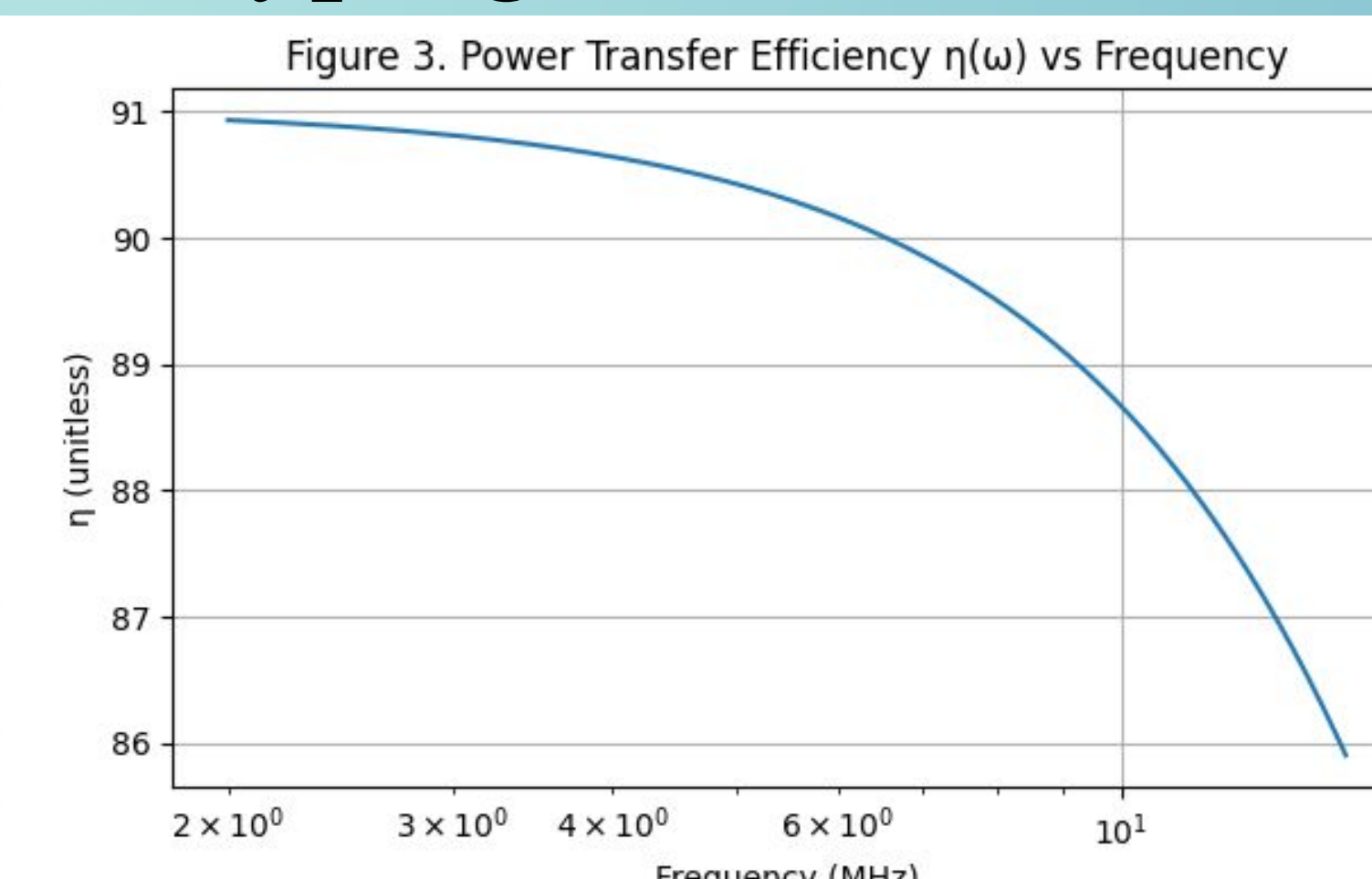


**Figure 3.** Phase of Zload frequency for the same representative case. Phase is computed from the complex Zload and relates to waveform distortion and reactive energy storage (capacitive or inductive)

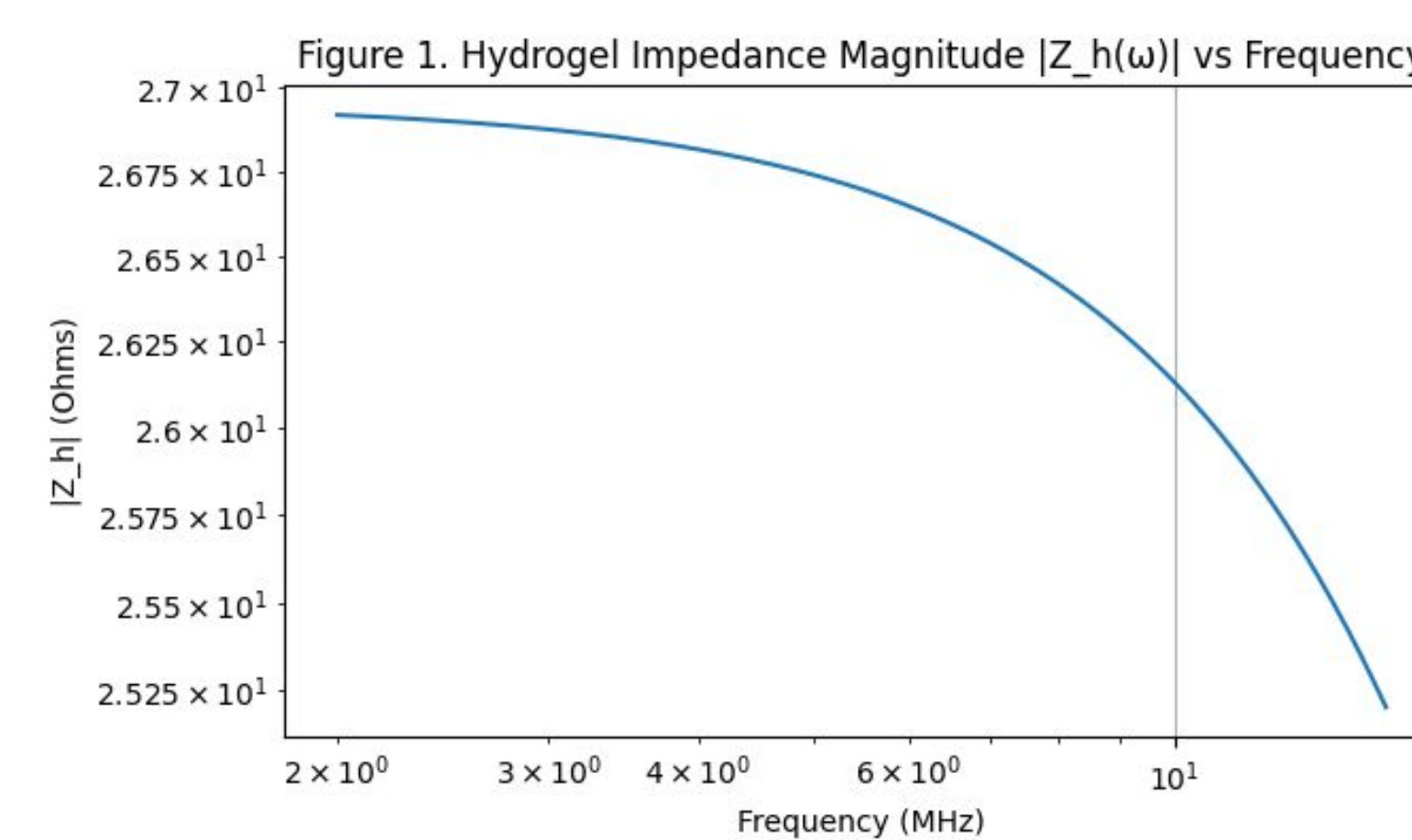


**Figure 4.** Cross-section of the probe-hydrogel-skin interface and equivalent circuit used in the model. The hydrogel is modeled as a lossy dielectric slab (thickness h, area A) with complex permittivity  $\epsilon h^*(\omega)$  and conductivity  $\sigma h(\omega)$ . The electronics reference impedance is  $Z_0$ , and the total series load  $Z_{load} = Z_h + Z_c + Z_{skin}$  is used to compute the reflection coefficient  $\Gamma(\omega)$  and power transfer  $\eta(\omega)$ . This circuit maps hydrogel design variables directly to the electronic matching metrics that control SNR in the imaging chain.

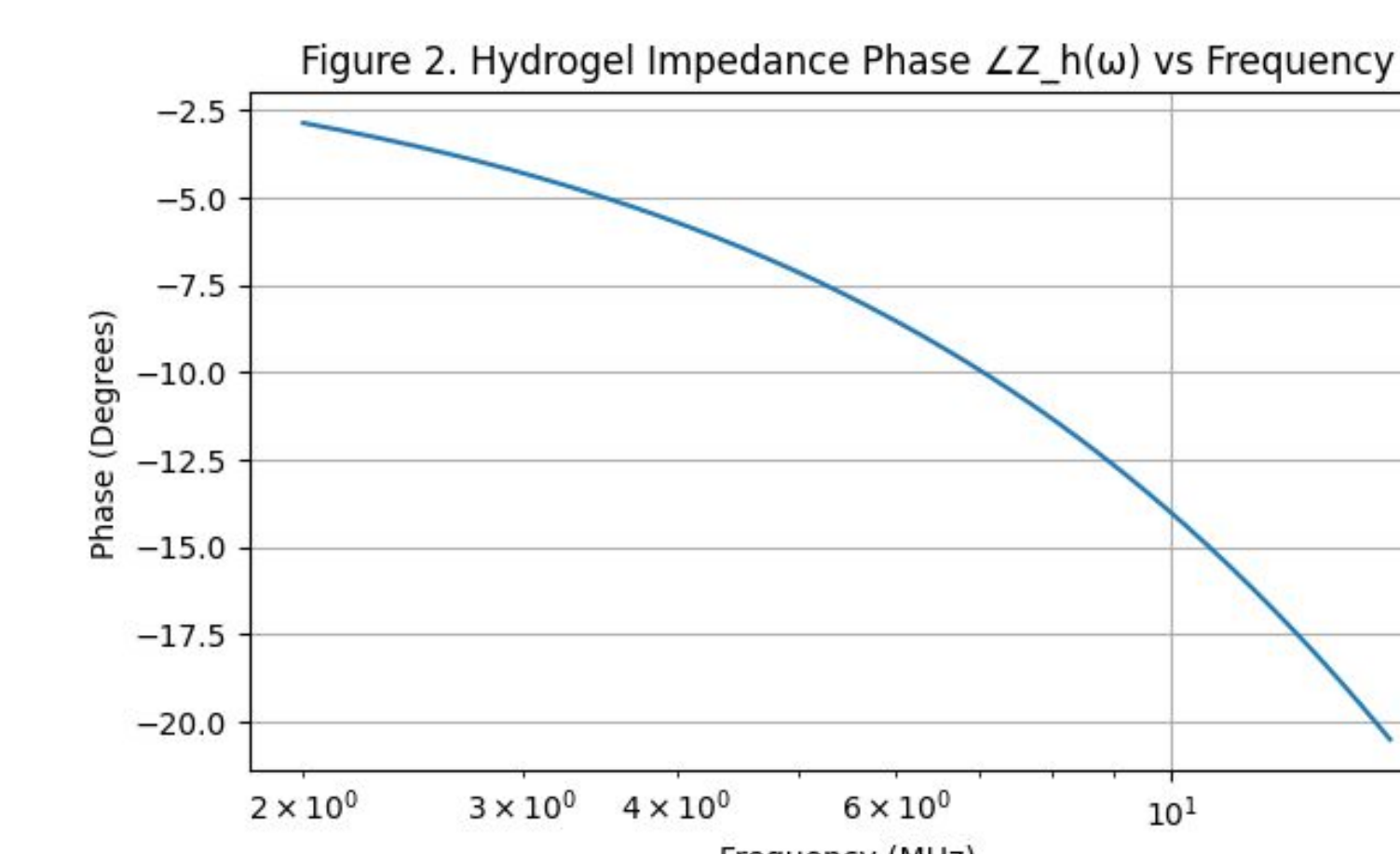


**Figure 5.** Frequency response of the total load magnitude  $|Z_{load}(f)|$  for a representative hydrogel formula. This plot was computed using Eq. (5) for  $Z_h$ , Eq. (8) for  $Z_{skin}$  (Cole-Cole informed parameters), and Eq. (6) to form  $Z_{load}$ . The curve shows how  $|Z|$  varies across the 2–15 MHz imaging band; the design goal ( $50 \Omega \pm 10 \Omega$ ) is plotted as horizontal bounds to visualize whether the formulation meets the CTQ across the band.

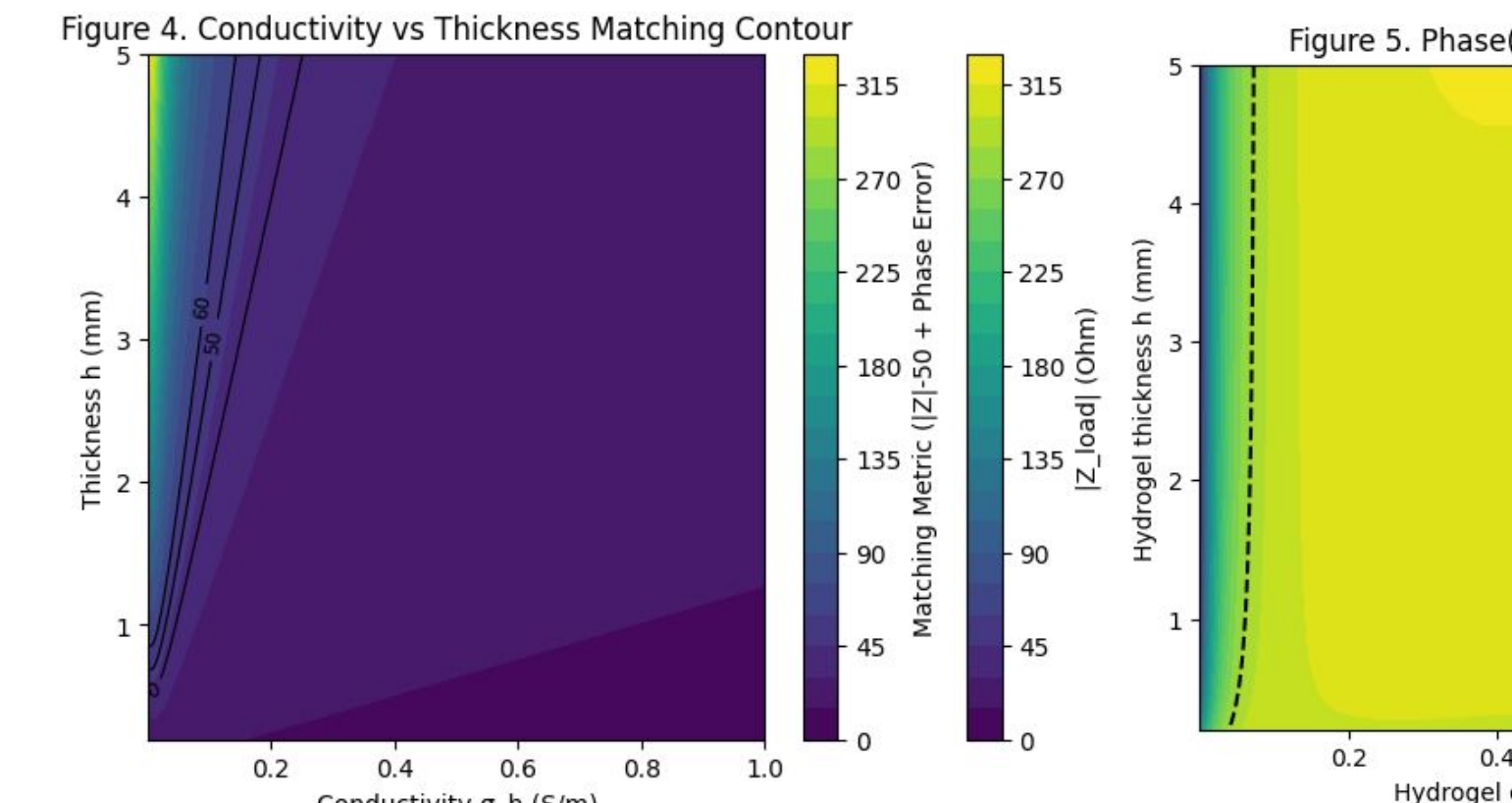


**Figure 6.** Power-transfer efficiency  $\eta(f)$  across frequency for the representative case. This figure illustrates how impedance mismatch reduces delivered power at specific frequencies, and hence how impedance tuning (adjusting  $\epsilon h$ ,  $\sigma h$ , or  $A$ ) trades off across the imaging band.

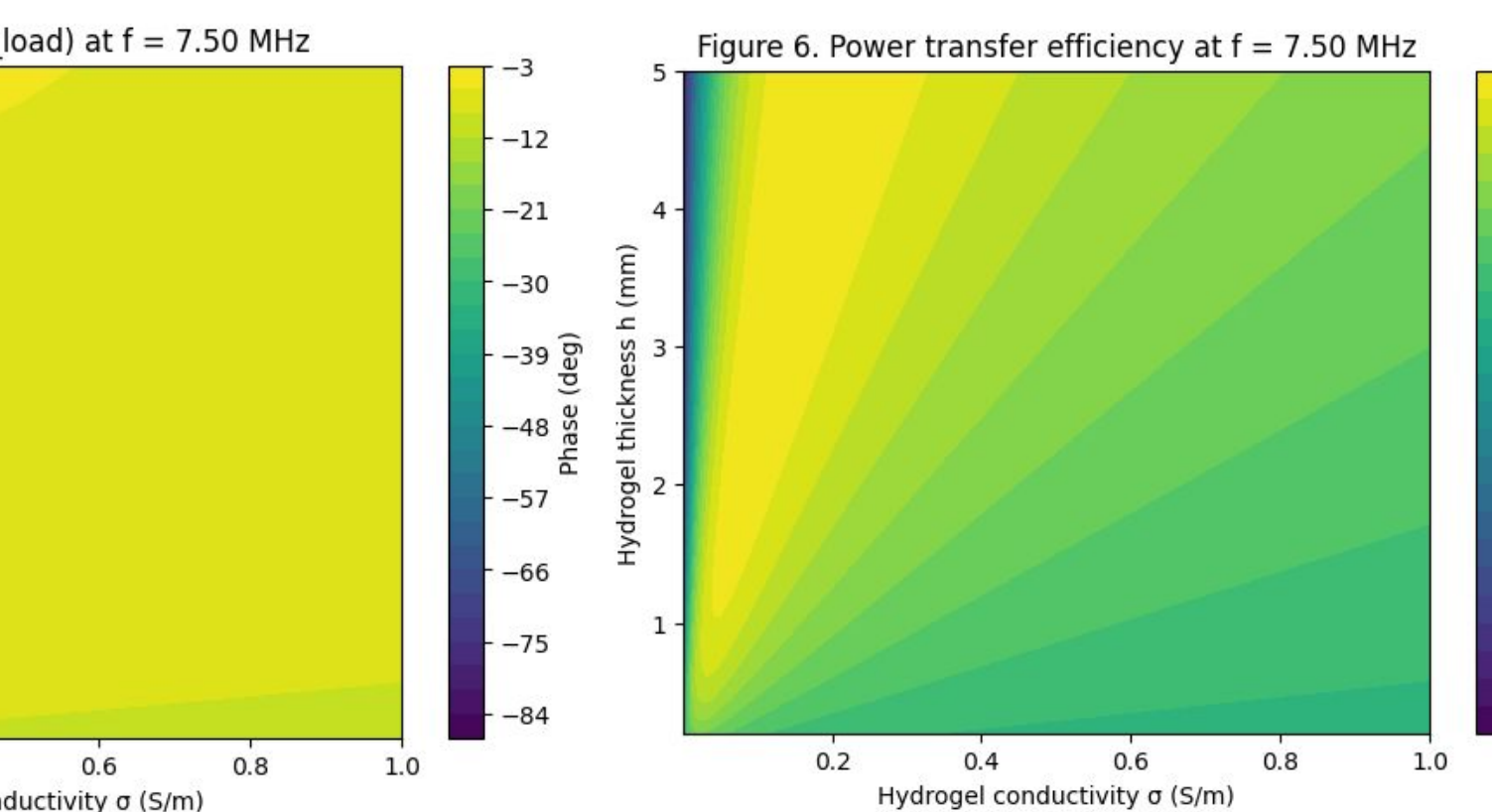


**Figure 7.** Contour map of  $|Z_{load}|$  at the center frequency (e.g., 7.5 MHz) as a function of hydrogel conductivity  $\sigma h$  (x-axis) and thickness  $h$  (y-axis). The contour overlay highlights the locus where  $|Z_{load}| = 40, 50, 60 \Omega$ ; the region between 40–60  $\Omega$  indicates combinations of  $\sigma h$  and  $h$  that meet the magnitude CTQ. This figure comes directly from the analytic form (Eq. 5) evaluated over a grid and is used to derive feasible formulation ranges.

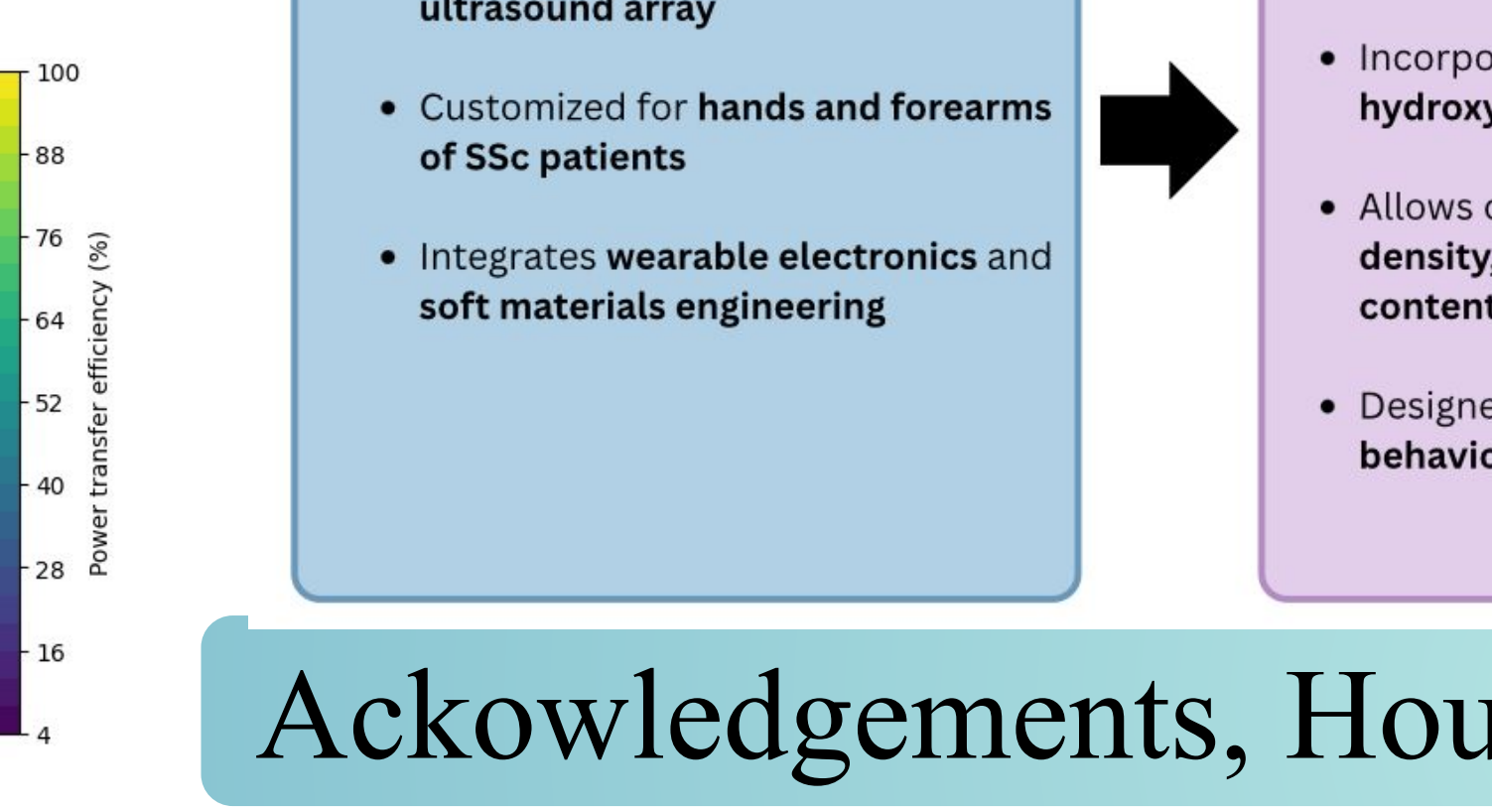
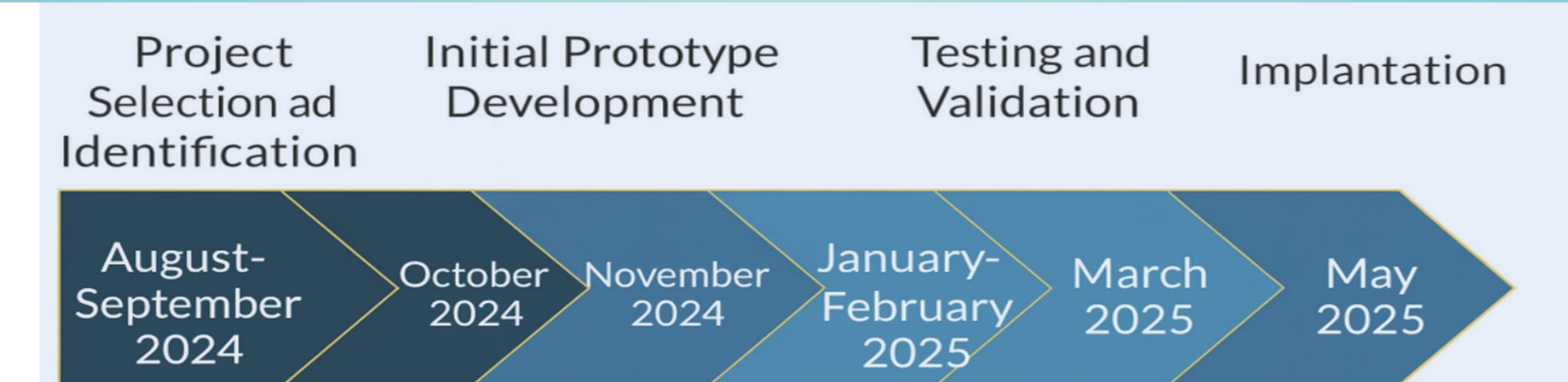


**Figure 8.** Contour map of phase of  $Z_{load}$  at center frequency vs  $\sigma h$  and  $h$ . This shows where the phase CTQ ( $\pm 15^\circ$ ) is satisfied and where it is violated; combined with Figure 5 it identifies the feasible design region that simultaneously satisfies magnitude and phase CTQs.

### Project Timeline



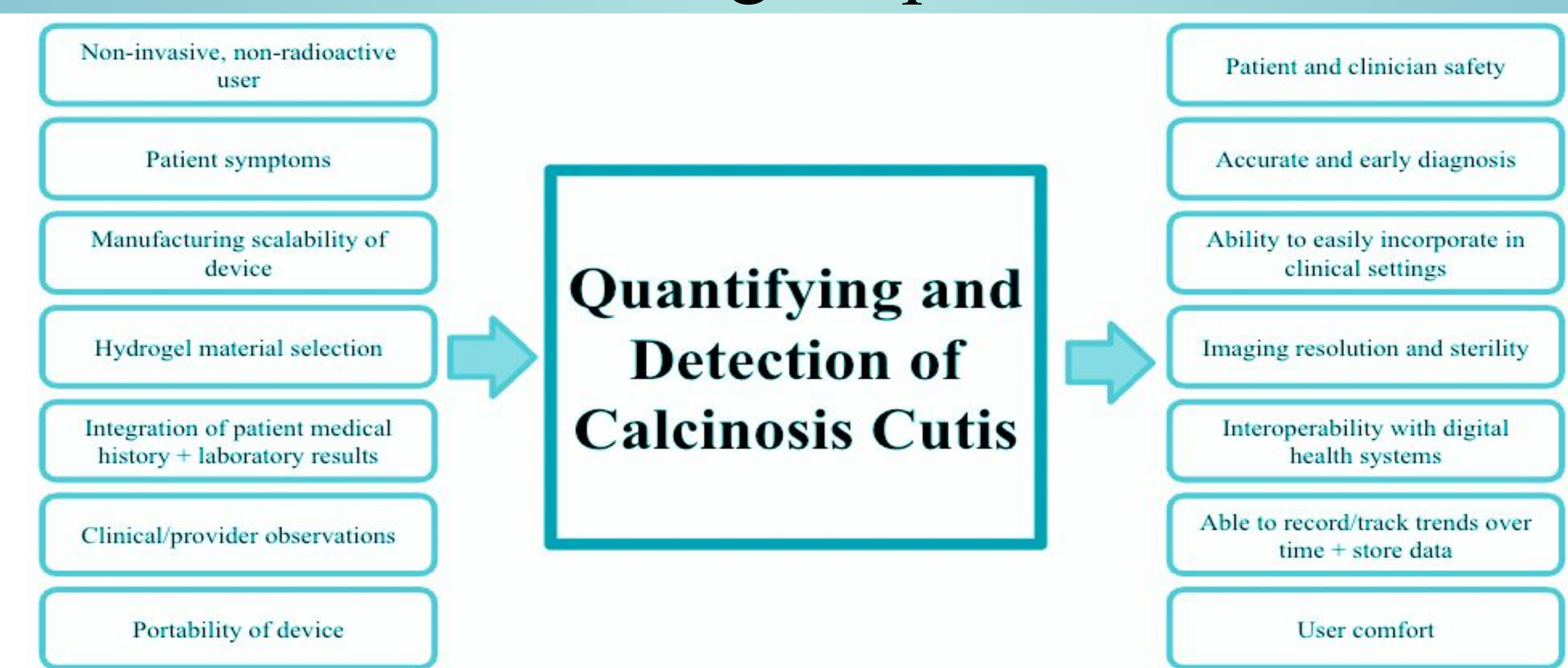
### Manufacturing Costs

Preliminary cost modeling supports a **per-unit disposable material cost of \$7.57 polyurethane sleeve** with dimensions of **7.5 x 0.4 x 7.5 in**. The raw material cost will depend on the market price of polyurethane gel, but is estimated around **\$1.57**. Manufacturing and additional costs (packaging, overhead, etc.) are estimated to be around **\$6.00**.

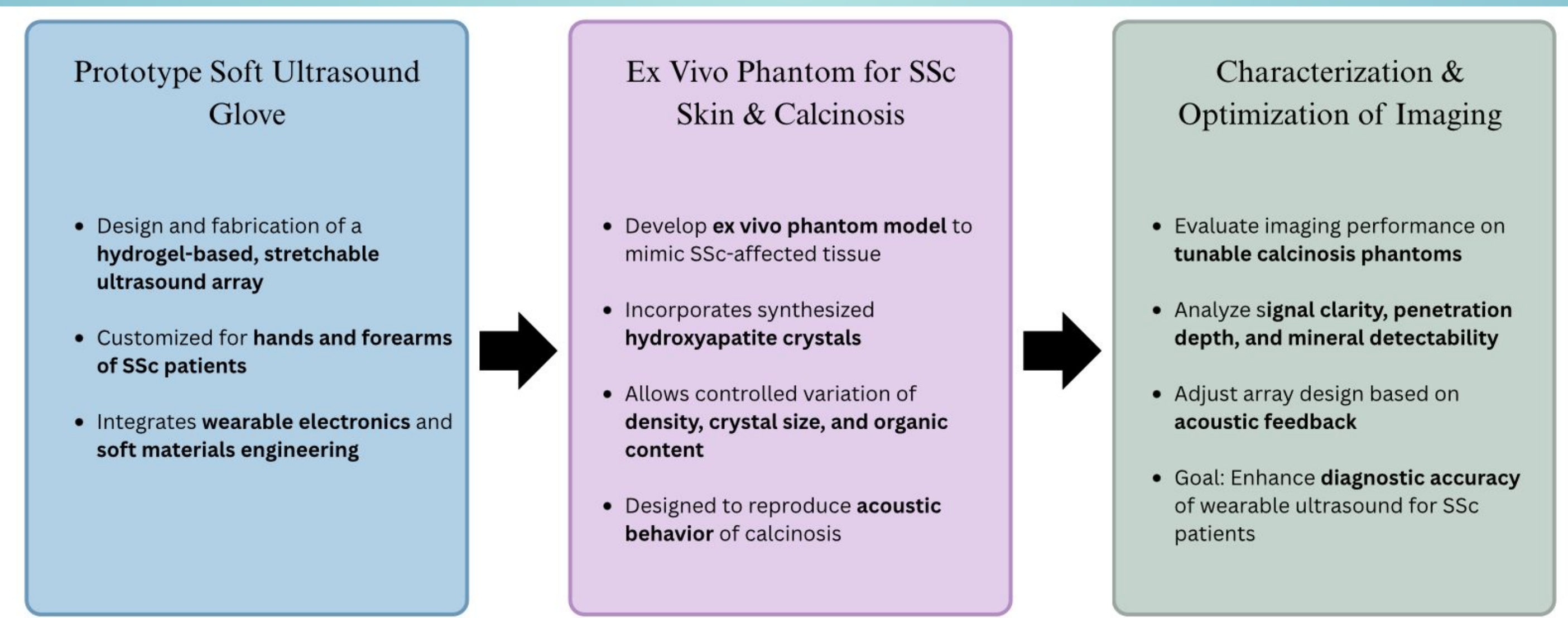
### Regulatory Pathway



### Design Inputs



### Future Directions



### Acknowledgements, House of Quality, and References

We would like to thank our mentors Dr. Nagaraja, Dr. Sohn, Dr. Verma, and Dr. Pham for their guidance, expertise, and support throughout this project. We would also like to thank Dr. Vernon, Professor Sobrado, and the rest of the School of Biological and Health Systems Engineering for providing us the opportunity and resources to pursue impactful engineering work.

